

# Modeling for Accurate Dimensional Scanning Electron Microscope Metrology: Then and Now

MICHAEL T. POSTEK AND ANDRÁS E. VLADÁR

Mechanical Metrology Division, National Institute of Standards and Technology, Gaithersburg, Maryland

**Summary:** A review of the evolution of modeling for accurate dimensional scanning electron microscopy is presented with an emphasis on developments in the Monte Carlo technique for modeling the generation of the electrons used for imaging and measurement. The progress of modeling for accurate metrology is discussed through a schematic technology timeline. In addition, a discussion of a future vision for accurate SEM dimensional metrology and the requirements to achieve it are presented. SCANNING 33: 111–125, 2011. Published 2011 by Wiley Periodicals, Inc.<sup>†</sup>

**Key words:** SEM, Monte Carlo modeling, metrology, accuracy, critical dimensions, electron–solid interactions

## Introduction

Scanning electron microscopes (SEM) have been used as quantitative measurement tools for a number of years. But, quantitative measurements with any scientific instrument require more care and understanding than one might first assume. The physical principles that dominate quantitative measurements must be fully understood and accounted for in the measurement. For

example, in optics, there are the effects of diffraction that must be overcome; in scanned probe microscopy, the scanned probe tip shape must be considered; and in scanning electron microscopy, the generation of the measured signal, beam diameter, sample charging, and the electron beam–specimen interactions all must be considered. Computer modeling and the associated experimental verifications to understand these issues for all three types of instruments have been developed. But, for this paper, only the evolution and future prospects of electron beam–sample interaction modeling using the Monte Carlo method for accurate dimensional metrology will be discussed.

## Need for Modeling

It was once said, “...if you want the *correct* measurement, put the sample in the SEM.” Unfortunately, in principle that is true, but, in practice Postek and Joy (’87) demonstrated that measurement with the SEM has inherent pitfalls. These can be quite significant and must be understood before either precise or accurate measurements can be made with that instrument. Later, Postek *et al.* (’93a) further demonstrated that accurate SEM calibration and error analysis was one of the major problems confronting microscopists, at that time. These problems needed to be overcome to obtain even precise dimensional measurements. With that knowledge, instruments and measuring methods improved tremendously and the quality of the imaging and the measurements has improved substantially.

The SEM image appears straightforward, but this could lead to misinterpretation, especially in metrology. The image is not a perfect representation of the sample, but rather approximately the convolution of the sample and the excited volume. Without properly accounting for the excited volume, it is impossible to obtain accurate results. The (often) micrometer-size excited volume is not negligible compared to the desired image and measurement resolution. Since the excited volume depends on the sample, which is the measurand, only inverse methods can be applied; hence, modeling must be used.

<sup>†</sup>This article is a US government work and, as such, is in the public domain in the United States of America.

Contribution of the National Institute of Standards and Technology; not subject to copyright. Certain commercial equipment is identified in this report to adequately describe the experimental procedure. Such identification does not imply recommendation or endorsement by the National Institute of Standards and Technology, nor does it imply that the equipment identified is necessarily the best available for the purpose.

Address for reprints: Michael T. Postek, Mechanical Metrology Division, National Institute of Standards and Technology, Gaithersburg, MD 20899

E-mail: postek@nist.gov

Received 8 March 2011; Accepted with revision 22 April 2011

In the beginning, scanning electron microscopists believed that irradiating a sample with an electron beam in an electron microscope rather than viewing it with an optical microscope provided an accurate depiction of the sample simply because the “resolution” was much better. Unfortunately, that is not the case, and many of the reasons for that will be discussed later in this paper. A clear understanding of the numerous factors that comprise and contribute to imaging and measurement uncertainty in an SEM is essential, and true dimensional accuracy can only be achieved through modeling of the *entire* measurement process. This process may be too involved or unnecessary for some applications, but to claim accuracy in an SEM-based dimensional measurement, modeling is essential. Figure 1 is an idealized depiction of the current SEM situation (Path A) and the ideal future situation incorporating modeling (Path B).

Until now, Path A has been the easier and more straightforward path to follow. This path has successfully provided a wealth of SEM-based images and measurements for many fields of science and technology, especially for the semiconductor industry. A well-calibrated, modern SEM instrument is capable of highly precise measurements due to many instrument improvements, and the magnification (or scale) can be accurately calibrated with a high level of confidence using the appropriate calibration samples. The precision of the measurements can generally be at, or better than, 0.2 nm ( $1\sigma$ ), and for many applications, such as semiconductor production, this high precision is adequate.

However, for an accurate measurement, precision is a necessary but not sufficient requirement. For

accuracy today, and more in the future, a proposed alternate path shown as Path B is the way to proceed. Path B incorporates image and instrument modeling. It is imperative to determine the *actual* structure from the collected image. Accomplishing that requires employing a tested and verified physics-based electron beam–sample interaction and signal-generation model. The overall model must also include modeling to account for instrument electronics’ pertinent characteristics (discussed below) and for sample charging. The images simulated by the model can be compared with the actual images from the SEM. Such a process will then reveal far more structural and dimensional information about the sample under test than is currently being obtained, and can provide an accurate measurement at a calculated level of uncertainty.

### Monte Carlo Modeling

The interaction of electrons with a solid is an extremely complex affair. In the electron microscope, on entering the sample, each electron may scatter several hundred times before escaping or losing its energy, and a million or more electrons per second may interact with the sample. Therefore, statistical techniques are appropriate means for modeling this interaction. The most adaptable research tool applied to this problem has been the *Monte Carlo* (MC) simulation technique (Myklebust *et al.*, '76). In this technique, the interactions are modeled and the trajectories of individual electrons are tracked through all regions

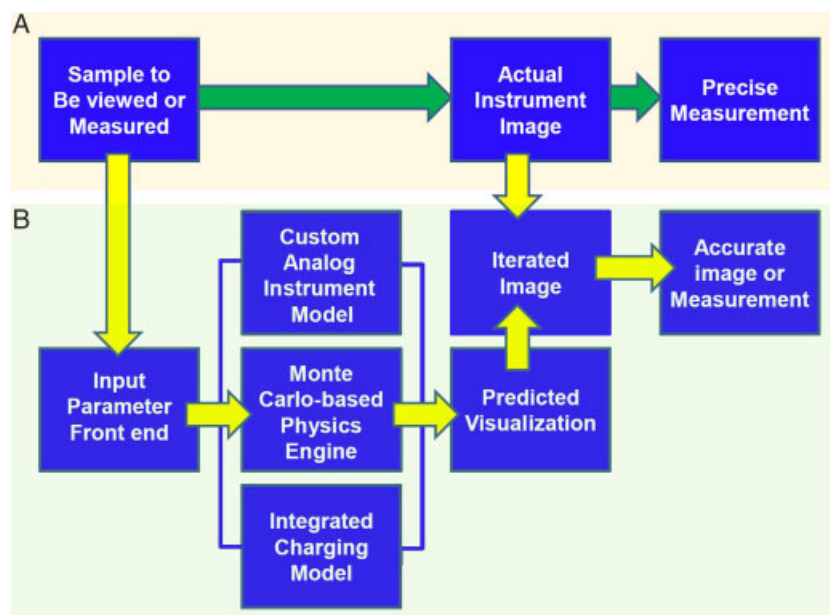


Fig 1. Idealized schematic depiction of imaging and measurement in the SEM current and projected future paths. SEM, scanning electron microscope.

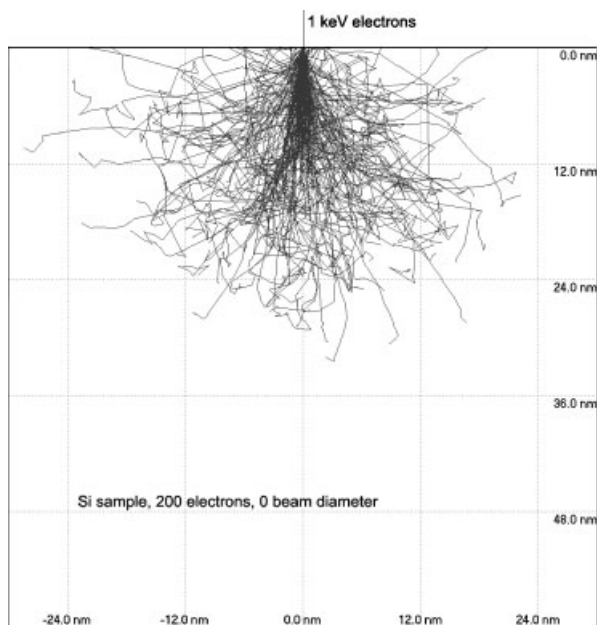


Fig 2. Example of Monte Carlo modeled primary electron beam-sample interaction for a single point in a Si sample.

of the sample (Fig. 2). Because many different scattering events may occur and because there is no a priori reason to choose one over another, algorithms involving random numbers are used to select the sequence of interactions taken by any electron (hence the name, Monte Carlo). By repeating this process for a sufficiently large number of incident electrons (usually 10,000 or more), the effect of the interactions is averaged, thus giving a useful idea of the way in which electrons will behave in the sample. The MC modeling techniques were initially applied to X-ray microanalysis to understand the physics and generation of this analytical signal. Today, the MC technique is being applied to the modeling of all signal-generating mechanisms of the SEM. The great benefit afforded by the MC method of simulation is that, using this technique, each electron is individually followed; everything about it (position, energy, direction of travel, etc.) is known at all times. Therefore, it is possible to take into account the sample geometry, the position and size of detectors, the size, shape, and intensity distribution of the electron beam, and other relevant experimental parameters of the primary electron beam. These input parameters can also be changed to investigate their effects on an image or measurement. Today, the computer required for these Monte Carlo simulations is unexceptional and current high-performance desktop personal computers can produce useful data in a reasonable time.

In its simplest and earliest form, the MC simulation for imaging allowed the backscattered electron (BSE) signal to be computed. BSE modeling only required the program to count that fraction of

the incident electrons that subsequently re-emerged from the sample for any given position of the incident beam. By further dividing these BSEs on the bases of their energy and direction of travel as they leave the sample, the effect of the detection geometry and detector efficiency on the signal profile could also be studied. However, while the information regarding the BSEs is a valuable first step, under most practical conditions, it is the secondary electron (SE) signal that is most often used for imaging and metrology in the SEM. Through the years, modeling has developed in an evolutionary manner as new science was generated and computing power improved. We have attempted to describe this through an idealized technology timeline (Fig. 3), which is discussed in greater detail below.

## Zero-Dimensional or Point Analysis Modeling

### Microprobe-Based Analytical Instrumentation

The historical starting point that prompted the development of this type of MC modeling was X-ray microanalysis. Therefore, in this article, zero-dimension (0-D) refers to point or spot mode since early microprobe-based analysis was a point-by-point analysis in the  $X$  or  $Y$  directions. Early microscopists doing X-ray microanalysis quickly found that there was a need for a greater understanding of the electron beam-sample interaction, excited volume and the generation of X-rays. There were initially other forms of modeling used to understand these phenomena but Monte Carlo modeling became the most common approach. Bishop ('76) reviewed the early history and development of modeling and traced the usefulness of the Monte Carlo technique in understanding the theory of X-ray microanalysis to Green ('63). Bishop also reported that by 1965 a number of workers demonstrated that more general approaches, based on theoretical calculations, could be used. This progress was spurred by the “computer revolution” (Bishop, '76) through the development of more “powerful” computers—powerful, that is, for that time in history. Early Monte Carlo modeling was used for the understanding the electron beam interactions for quantitative X-ray microanalysis, where the depths from which the X-rays induced by the primary electron beam were generated needed to be known with some degree of certainty. Key contributors to this topic, among others, included David C. Joy, Kurt Heinrich, Dale Newbury, Robert Myklebust, and David Kyser. Much of this early work is summarized in the Proceedings of a workshop held at the National Bureau of Standards in 1975 (Heinrich *et al.*, '75), in the 1982 Proceedings of the First Pfefferkorn Conference (Kyser *et al.*, '82), Kyser ('81) and in Joy

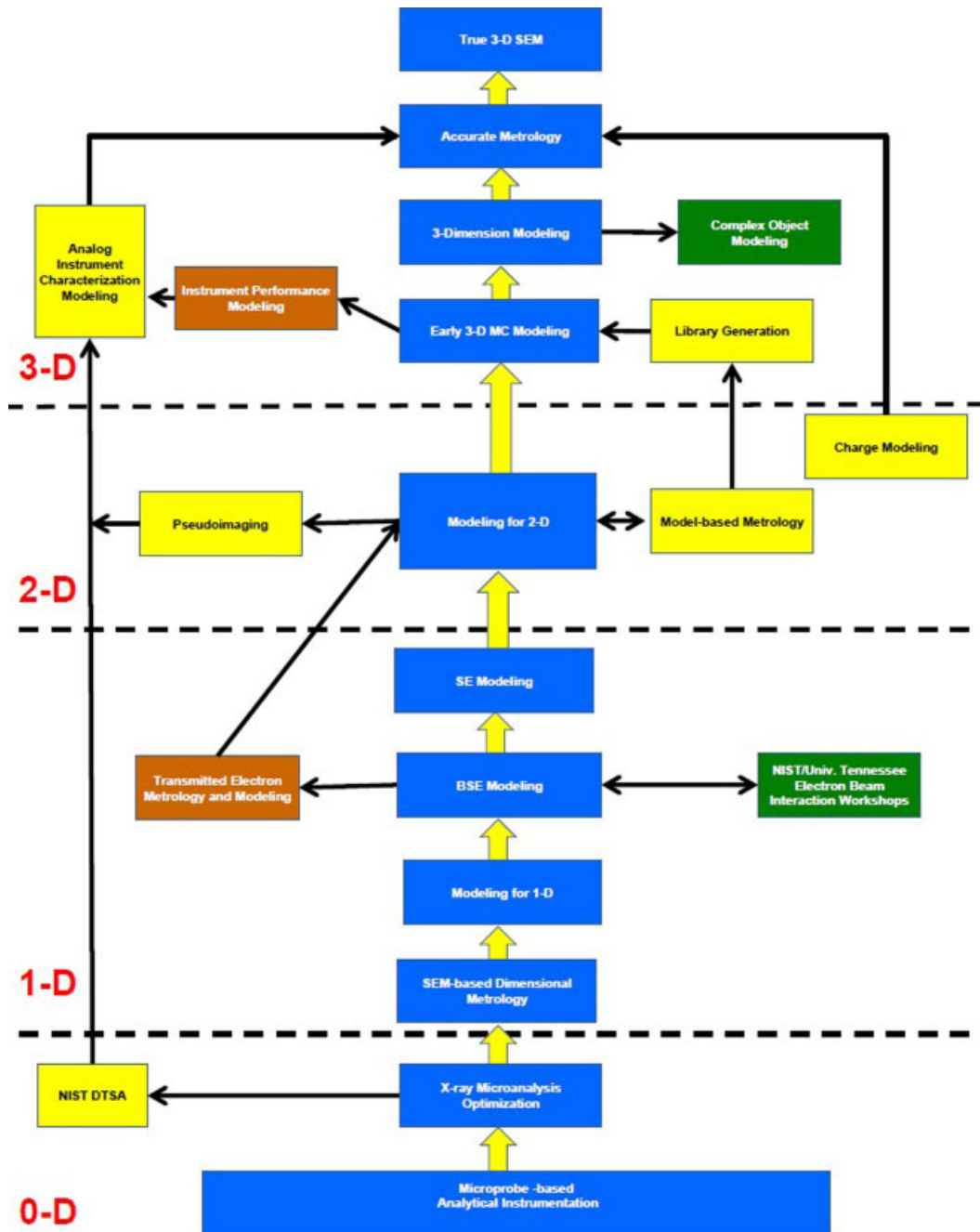


Fig 3. Idealized technology timeline for SEM dimensional metrology modeling. SEM, scanning electron microscope.

(’95). Monte Carlo modeling became the tool for understanding X-ray generation and instrument parameter optimization.

**X-ray Microanalysis Optimization**

The early Monte Carlo programs provided good information about the derivation of X-rays and contributed a great deal to the development of X-ray quantitative microanalysis. One of the very useful early tools for understanding and experimenting for microanalysis was the NIST DeskTop Spectrum Analyzer (DTSA) program (Fiori *et al.*, ’91). Although not

based on MC, this program helped to shape much of the fundamental thinking about instrument-induced effects on the data being acquired. DTSA was exclusively aimed at X-ray spectrometry and both EDS and WDS spectrometers could be explicitly modeled, including: EDS efficiency (both Si and Ge based detectors were considered), the detector solid angle, the window materials, the potential for an ice layer build-up on the detector face, the first surface electrode, the Si “dead” layer, the detector absorption response function (including transmission through the detector), and finally the EDS peak broadening function. This proved to be uniquely valuable to the understanding

and the interpretation of X-ray microanalytical data. Where dimensional metrology was concerned, this program provided a clear demonstration that detrimental signal modifications can be induced by the instrument's electronics and become embedded into any quantitative metrology data. The NIST DTSA program has evolved over time and a new, fully revised version of the classic (named DTSA-II) has been developed and released now including an embedded Monte Carlo for calculation of EDS spectra from a variety of specimen geometries (Ritchie, 2011). Similar instrument and electronics modeling must be incorporated into the modeling for SEM dimensional metrology, as well.

## One-Dimensional Modeling

### SEM-Based Dimensional Metrology

It is likely that one of the first questions asked when the first SEM micrograph was initially viewed was “how big is this?” Initially, relatively precise, but highly inaccurate measurements were made, one way or another, in an SEM. Techniques included using a ruler (likely made of flexible plastic) to measure directly from the viewing cathode ray tube (CRT); on-screen cursors, or from the actual “Polaroid” or photographic print. Line scans and other measuring systems were also utilized, but all these methods had numerous areas of weakness (Postek *et al.*, '93a). Owing to the relatively large size of the structures and low magnifications involved, at that time, this did not pose a big problem since a large measurement uncertainty was acceptable. Today, many semiconductor structures are in the sub-50-nm range, which can place them on the same scale or smaller than the electron beam interaction zone.

Late in the 1980s, it became apparent that the SEM would be used as an on-line measurement tool in semiconductor manufacturing as “Moore's Law” (Moore, '65, '95) pushed the device critical dimensions below 0.5  $\mu\text{m}$ . Semiconductor manufacturing companies pushed the instrument manufacturers to develop fully automated on-line critical dimension (CD) measurement scanning electron beam instruments. With those instruments, better approaches to making measurements with the SEM began to become available, especially with the development of digital measurement systems and frame averaging to improve the signal-to-noise ratio. As computers became faster, the modeling capabilities also became more sophisticated and scaled with the computing power now available in desktop computers. This freed the workers to begin to adapt MC computer code for the development of more accurate models to understand the signal mechanisms composing the SEM images.

### Modeling for 1D

Early experimental and modeled data demonstrated that as the electron beam enters into a sample, scattering begins, and depending upon the energy of the electron beam and the materials being irradiated, the depth of this penetration and the amount of scatter is variable. Figure 2 illustrates this by showing a small number of MC modeled electron trajectories in a generic material. If given enough time and electrons, the tracks form a 3-dimensional, generally “tear-shaped” volume. This behavior and interaction has been experimentally verified by Everhart and Hoff ('71) and Everhart and Chung ('72). Conventional MC modeling at that time sought to explain this behavior and to describe the x-ray generation location distribution, and the backscattered electron signal (more readily modeled than the secondary electron signal). This was accomplished by graphically displaying the calculated backscattered electron signal from several point analyses of a number of discrete locations across a simple geometric structure. Due to limitations in the computing power, this was generally displayed as a simple 1-D representation of position vs. collected signal (Fig. 4) as a cross-sectional view. Early workers employed large super computers to provide sufficient data to achieve good sampling statistics and signal-to-noise ratio.

Joy (Joy, '82; Joy *et al.*, '82) was one of the first to suggest and demonstrate that Monte Carlo electron beam-sample interaction code could be effectively run on a desktop personal computer and he began to re-work and optimize his code accordingly. Joy and other workers clearly demonstrated that even though the supercomputers have their advantages, one main disadvantage is that they share central processing unit (CPU) time among a large number of users. Thus, the fast computing power is reduced by the number of users also running complex programs. Owing to the reasonable cost, dedicated personal computers (which were, at that time, lower in overall speed than supercomputers) proved to be competitive because they could be programmed to dedicate 100% of the CPU time to the MC calculations. Because of the open and freely available MC code from David C. Joy (and others), the Monte Carlo method became more popular and the tool of choice for understanding electron beam interactions (Joy, '84, '89, '91, '95; Joy *et al.*, '86a,b; Czywewski and Joy, '89). It should be noted that the MC method is not the only method for modeling for metrology that has been proposed. Nyssonen ('88) proposed a surface integral of a probability density function model and Hatsuzawa ('93) proposed a cylindrical envelope projection model. However, the MC modeling has been the most commonly employed.

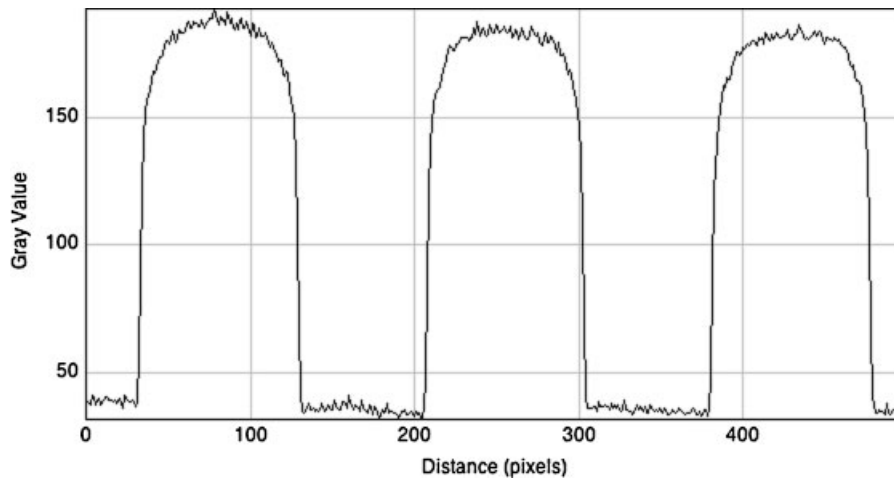


Fig 4. Backscattered electron line scan of three silicon lines modeled with Monte Carlo method as signal vs. electron beam position generated at 512 points at zero beam diameter.

### BSE Modeling

One-dimensional (1D) Monte Carlo modeled data acquired and displayed, as stated earlier, typically take the form of a linescan or a 1D representation of signal collected vs. position of the impinging beam (Fig. 4). High-energy BSE images began to visually represent the specimens being analyzed but only in cross-section view (Fig. 4). But, although limited, by today's standards, these data did provide a wealth of information about electron beam/specimen interactions. The BSE signal proved to be readily modeled and demonstrated the value of continuing on to the next logical step—*SE modeling*.

Measurement of the energetic BSEs for dimensional metrology was shown experimentally, and also through modeling, to be more precise when compared with the SE signal. This is a result of reduced charging and edge “blooming” effects characteristic of the SEs (Postek, '90). The rapid increase in SEs as the primary electron beam scans near an edge actually masks the edge and broadens the measurement using typical edge detection algorithms. Recognizing this, an early CD SEM was built around this concept (see: Metrologix). The instrument proved to have very high measurement precision. Unfortunately, throughput was lower than the industry desired because of the increased data collection time needed to acquire sufficient information from the BSE signal on photoresist and other low atomic number semiconductor materials. For high throughput, the SE signal became the signal of choice and will be discussed further below.

### Transmitted Electron Metrology and Modeling

The transmitted electron (TE) signal, like the BSE signal, proved to be an excellent subject for Monte

Carlo modeling. With a suitable sample, the TE signal generation is simple and it can be collected a number of ways in an SEM. The TE signal has not been exploited as much as SE and BSE signals for dimensional metrology, but early applications demonstrated the value of modeling using this signal mode. It also provided significant evidence supporting the importance of modeling, in general.

TE was proven useful in the study of one early semiconductor industry sample of interest—X-ray lithographic masks. X-ray masks can have electron (and X-ray) dense and electron (and X-ray) transparent regions. Those areas inhibiting the transmission of the X-rays and hence the lithographic pattern are commonly composed of electron dense gold structures on a thin Si membrane. Those areas of the membrane not patterned are electron transparent at high accelerating voltages. Therefore, a high-contrast TE signal can be collected and measured. Modeling of the multilayer X-ray mask and the TE signal proved to be straightforward (Lowney *et al.*, '96) and also provided a unique opportunity to demonstrate how a specimen–electron beam interaction experiment could take advantage of MC modeling.

Figure 5 shows the results of Monte Carlo modeled “X” linescans of an X-ray mask TE signal (inverted) modeled at 160 points along the scan with 1,000, 2,000, 5,000, 10,000, 20,000, 50,000, 100,000, and 200,000 electrons per point. The noise, the square root of the number of electrons, expressed as the percentage of the full scale is 3.2, 2.2, 1.4, 1.0, 0.7, 0.4, 0.3, and 0.2, respectively. At the time when these results were calculated, using a computer equipped with an Intel<sup>®</sup> 486 microprocessor, it took approximately 1 week to calculate the results for a field-of-view of about 2  $\mu\text{m}$ . The average pixel distance between modeled sample locations was approximately 13 nm—clearly not very high resolution. To achieve better resolution at the critical

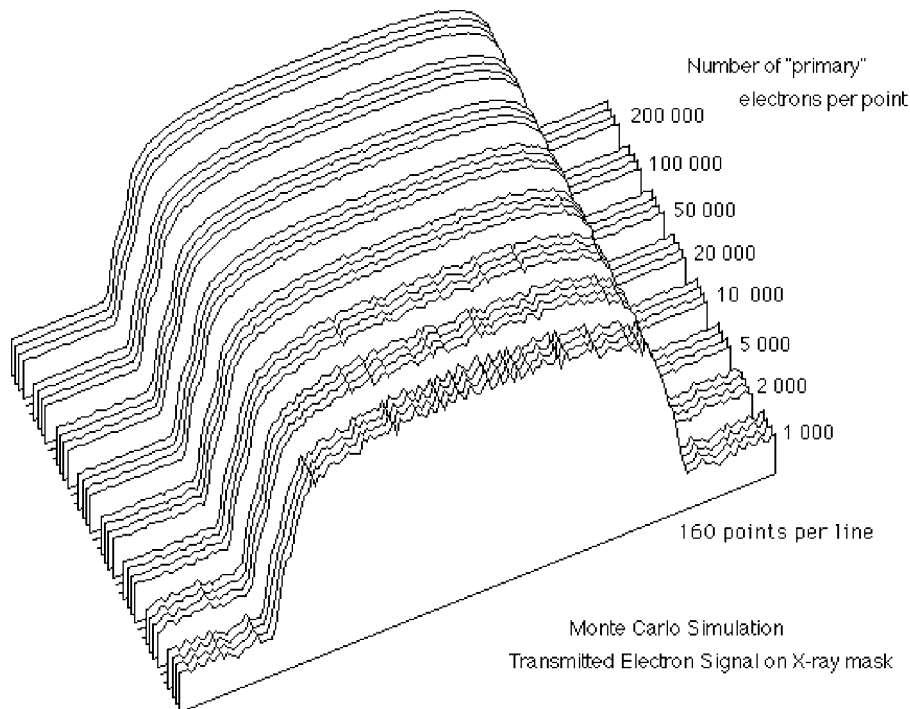


Fig 5. X-ray mask scanning transmitted electron signal (inverted) modeled at 160 points along the scan with various numbers of electrons per point.

part of the linescans and reduce computation time, the distances of the calculated data points were chosen to be variable. Employing this clever technique, at the regions of interest, such as those near the edges, more data was taken, and at areas of lesser interest, such as the substrate, fewer data points were taken. Also, due to early computer limitations, it was assumed that the left and right edges were symmetrical, and only one edge was calculated. After the initial computations, the other symmetrical half-linescan was added to get a whole linescan, as displayed.

The significant point of this work was the demonstration that modeling of the TE signal revealed that a great deal of more information is contained in a micrograph than had been considered before. In the TE modeled image, the modeling pointed out the presence of a small detail, a notch on the sidewall of the linescan. This detail should also be present in the TE image. Experimentally, this notch was not initially noticed because of resolution and signal-to-noise problems associated with early SEM instrumentation. However, optimizing the instrument operating parameters (reduced working distance and use of a high-resolution cold field-emission electron source) revealed the presence of the notch in the experimental data, as well. Figure 6 shows modeled and experimental images of an X-ray mask. In Figure 6 (upper), the modeled notch structure is apparent and in Figure 6 (lower) it can be seen that the notch structure (discussed above) is

experimentally resolved. The predicted presence of the notch through modeling preceded the ability to resolve the structure.

Interpretation of these data was that the size of the notch was directly related to the electron beam impinging on the sidewall of the gold line. This proved to be highly reproducible and an excellent place for the automated algorithms to precisely determine the linewidth (Postek *et al.*, '89, '93b). Although this methodology (with some further work) could have led to accurate X-ray mask standards, this lithographic technique went out of favor within the semiconductor industry because of the difficulty in manufacturing the fragile X-ray masks and the continual improvement of optical lithography. The TE was also found to be useful in the metrology of Scattering with Angular Limitation Projection Electron Lithography (SCALPEL) masks (Farrow *et al.*, '97; Liddle *et al.*, '97) which subsequently met a similar fate. Today, with the need for accurate nanometrology, this technique may again be valuable.

#### NIST/Univ. Tennessee Electron Beam Interaction Workshops

It became apparent in the mid-1990s, that there was a proliferation of 1D and a few two dimensional (2D) electron beam Monte Carlo codes being independently written, but most of them stemmed from the original X-ray Monte Carlo code. In 1994,

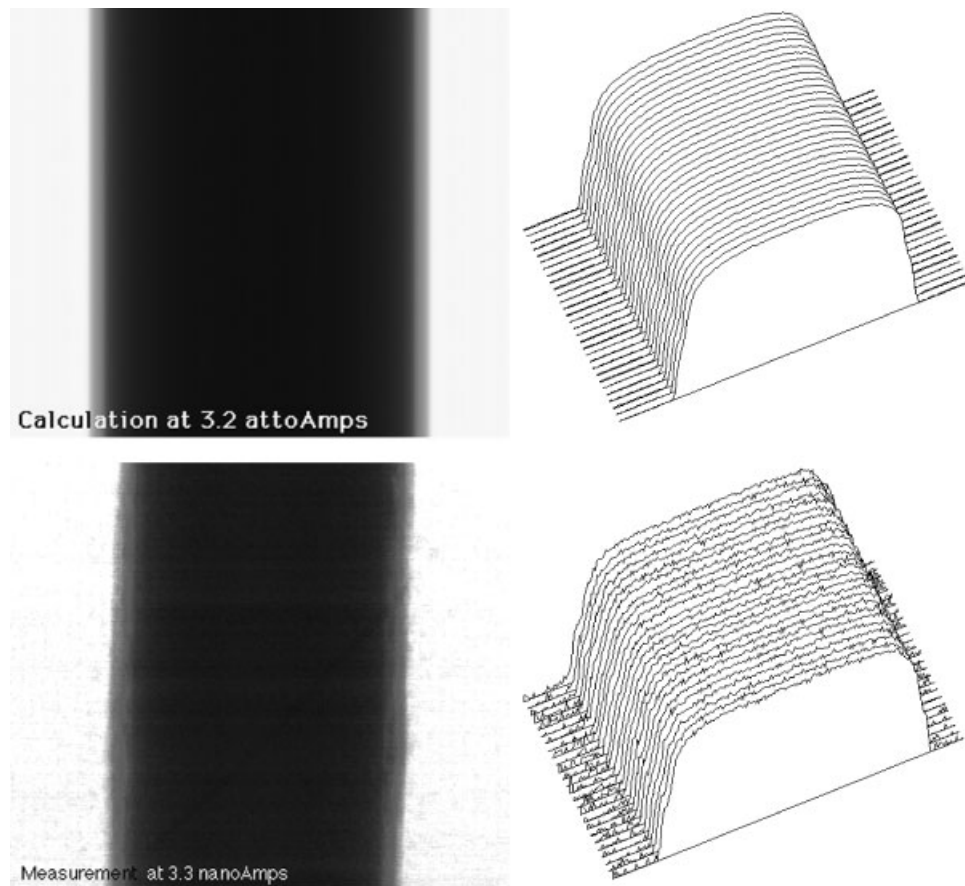


Fig 6. Modeled (upper) and real (lower) images of an x-ray mask (left) and inverted line scans in isometric view of the signal intensity (right) with the notch at the sidewalls clearly discernable.

the first Electron Beam Interaction Workshop was held, for the first time, at the 1994 SCANNING meeting. Modelers from around the world participated to meet and collaborate. At that Workshop, the participants felt that a modeling round robin should be started to compare computer code results. A structure to be modeled was identified and the experimental verification procedures were defined. This material was a rudimentary  $1\ \mu\text{m}$  step on a silicon wafer. The participants met again at the 29th annual Conference of the Microbeam Analysis Society where the results were documented and presented (Postek *et al.*, '95; Lowney *et al.*, '95a,b). It was found that there were differences in the MC results and the workers began to work collaboratively to resolve any differences in these data. This workshop and its offshoots unified the modeling community and proved to be critical to the success of the MC modeling efforts and allowed this method to progress at a much more rapid pace.

### SE Modeling

SEMs typically collect the “secondary” electron image. Hence, the ultimate goal was, and still is, to

accurately model the “secondary” electron image in order to accurately determine where the actual edges to be measured are found in the image. This is a fundamental research challenge requiring advancements in theory, as well as, instrumentation. It is known that the “secondary” electron image is a composite of several contributions: The SE-I component of the signal originates at and near to the location of the interaction of the primary electron beam on the sample, and depending upon instrument conditions, sample composition and topography, the generation of this signal can be from rather deep in the sample. The SE-II component is composed of secondary electrons that are generated by backscattered electrons re-emerging from the sample. These electrons represent a high portion of the total signal collected and can originate micrometers from the initial point of interaction of the primary electron beam (Hasselbach *et al.*, '83). The SE-III component of the signal originates from interactions of the high energy backscattered electrons with instrument components within the microscope chamber. This signal is sufficiently high that a mode of electron collection called converted secondary backscattered electron (CBSE) was developed to exploit it (Moll *et al.*, '78, '79). The SE-III signal



component varies significantly with instrument and final lens design and has been shown to be a major component of the SEM signal both at high and low accelerating voltages (Postek *et al.*, '88). The SE-IV signal component originates from primary electron beam interactions and the final lens components, such as apertures, and in more modern microscopes that source has been reduced substantially by improved final lens designs. In addition, any BSE whose trajectory is in direct alignment with the SE detector is also summed into the total signal. Therefore, the SE signal is highly complex and is a composite of a number of contributions (Peters, '82, '85). This fact makes accurate MC modeling of the SE signal highly complex, as well.

The complexity of the SE signal is mirrored by the slow, but progressive, nature of the MC modeling efforts. The MC modeling of the secondary electron signal has evolved a great deal over the years as greater knowledge about this signal mechanism was discovered and better experimental procedures to obtain these data were developed. Joy ('82, '85) produced, and made publically available, one of the initial SE modeling codes. The National Bureau of Standards/NIST developed the MONSEL series of programs (Lowney and Marx, '94; Lowney, '95a,b, '96a,b; Villarrubia *et al.*, 2001, 2003) and additional MC codes such as CASINO became available (Drouin *et al.*, '97, 2007; Hovington *et al.*, '97).

## Two-Dimensional Modeling

### Inverse Modeling

2D modeling provides MC information in an easy-to-understand, visual form, and makes visual comparisons between theory and experiment possible. More importantly, it makes it feasible to fully

evaluate various image processing and edge detection algorithms by the use of well-controlled images. These images can be generated with known types and amounts of imperfections common in real SEM images (i.e., beam diameter, noise, blur, astigmatism, and others). Fortunately, dimensional metrology of semiconductor lines requires modeling of relatively simple structures represented in the most important cases by single or multiple (isolated or dense) photoresist or polysilicon lines. High speed and repeatability of the so-called critical dimension (CD) measurements are essential for efficient production of integrated circuits (IC). The instruments used for this work generally are equipped with proprietary measurement algorithms, and testing these algorithms with modeled data ensures that the parameters of interest are being precisely measured. Generally, the smallest linewidth is the CD, which corresponds to the gate length, one of the most important parameters for the millions of transistors composing modern ICs. Therefore, the better the instrument measurement parameters are known, the better the measurements.

2D Monte Carlo modeling in its simplest form essentially arranges a series of 1D "X" linescans (Fig. 4) into a 2D matrix by replicating the same linescan in the "Y" direction. This results in a digital "artificial" image, which with the addition of noise and alphanumeric characters, can appear very similar to a real SEM image (Fig. 7). As the capabilities of the computers improved, faster Monte Carlo algorithms were devised and implemented. Soon, it became feasible to acquire X and Y data for the entire images of very simple structures. Earlier, in principle, this was possible, but the calculations of the required approximately quarter million to many million data points to obtain a meaningful SEM image was simply beyond the resources of most metrologists.

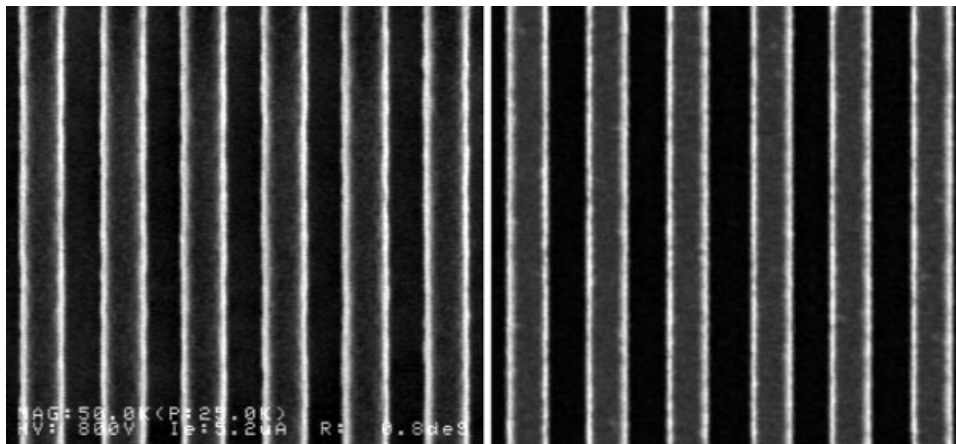


Fig 7. Comparison of SEM images from a (left) CD SEM and a modeled (right) image of dense resist lines. The modeled image has instrument characteristics such as those described in the text included in the image. SEM, scanning electron microscope.

Figure 7 demonstrates how similar a MC-modeled image of dense photoresist lines can resemble an actual SEM image. The modeled image, as described in Postek *et al.* (2002), was created by generating a high-resolution single “X” linescan in the NIST MONSEL program. Then many of these “X” linescans were replicated as described above to make a high pixel-resolution artificial SEM image. The initial modeled image (Fig. 7 right) was “perfect,” i.e., free of noise, blur, astigmatism, etc. A set of thorough physical measurements of CD-SEM input parameters was then made, which yielded the adjustments necessary and input parameters to convert the “perfect” modeled image into the artificial micrograph shown image (Fig. 7, right). The modeled, artificial image is indistinguishable from the real image the SEM can provide (Fig. 7, left).

In the CD-SEM, the acquired image data (or a segment of the image data) is typically analyzed using a manufacturer supplied (and often proprietary) measurement algorithm (i.e., threshold, regression, etc.). These various edge detection criteria used for present SEM linewidth measurements are somewhat arbitrary and, at best, are usually not on a firm theoretical foundation. The MC-generated artificial images can be used to test the applicability of these algorithms to the measurement task. Table I shows the results of the application of several common algorithms to the measurement of a simulated palladium on silicon line image prepared like as those described above (Postek *et al.*, 2002). Note how different the measurement results are between the different algorithms that have been applied (variation in pitch measurements can be attributed to pixel size and induced line edge roughness). A simulated image is extremely valuable in this measurement because all the input parameters to the simulated image are known. Hence, the pitch, linewidth, and space width are accurately known. A similar discrepancy among width measurements was demonstrated in the SEM Interlaboratory Study using experimental data (Postek *et al.*, '93a). To accurately determine where, on the intensity profile, the measurement of width should be made, an accurate MC model is required. In addition, the characteristic parameters of laboratory and production SEMs vary with the type and manufacturer

TABLE I Comparison of common measurement algorithms applied to a modeled image

Algorithm	Space width (nm)	Linewidth (nm)
Peak	109.5	91.2
Threshold	91.7	110.6
Regression	75.6	125.9
Sigmoid	92.9	110.5
Actual	105.8	96.6

of the SEM and its operating conditions. For accurate modeling, all these factors must be taken into account (Radi *et al.*, 2003).

Over time, the performance of MC modeling has reached a level such that today it is possible to generate very convincing-looking two-dimensional artificial SEM images. Still, it takes a fair amount of time to run hundreds of millions of electrons through the calculations, especially if secondary electron images are used for the measurements.

### Model-Based Metrology

As stated earlier, the SEM image is approximately the convolution of the sample and the excited volume. Figure 8 schematically illustrates how Monte Carlo modeling can be used to extract information from this convolution, with a technique called “model-based metrology.” In this simple example, the sample has a rectangular cross-section (Fig. 8, upper left). However, the recorded image of the SE signal appears far different because of the increased generation of SEs as the beam approaches an edge (Fig. 8, upper right) forming the “typical” SEM image with bright edges. Modeling then accounts and corrects for the beam size and shape and the enhanced yield at the corners (Fig. 8, lower left). The size and shape of that rectangle can then be deduced from the linescan (Fig. 8, lower right). Model-based metrology shows that without properly accounting for the excited volume using modeling, it is impossible to obtain accurate results, especially when the excited volume is about the same size as the desired measurement resolution.

### Library Generation

The power of model-based metrology can be improved and sped up by the use of pre-computed libraries. This concept has been demonstrated in many instances and several various software solutions were developed over time. The so-called inverse scattering method that used commercially available MC software to generate a library of linescans and a fast algorithm to find the best match to the measured linescan was published by Davidson and Vladár ('99) and Gorelikov *et al.*

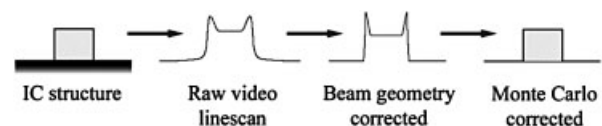


Fig 8. Schematic illustration of the steps of model-based SEM dimensional metrology, as described in the text. SEM, scanning electron microscope.

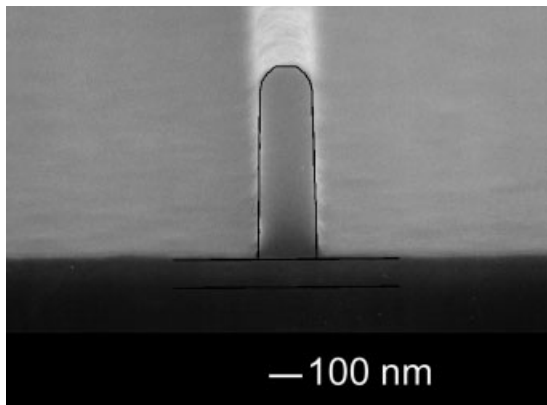


Fig 9. MC-modeled contour of an isolated resist line overlaid on its cross-sectional image showing the fidelity that can be obtained with modern MC programs.

(2005). Villarrubia *et al.* (2001, 2005) demonstrated that by using such an approach the precision of CD measurements could be improved by a factor of 3x, and information beyond just the width of the line, such as side wall angles, corner rounding, and feature height could be calculated with good certainty.

It must be understood that, rigorous MC 1-D and 2-D modeling must account correctly for many factors including proximity effects, i.e., for lack or presence of neighboring structure. When all these factors are properly applied, a well-developed MC model can correctly predict the shape of a semiconductor line, as shown in Figure 9 and by Villarrubia *et al.* (2003).

### Modeling of Sample Charging

The majority of samples to be viewed or measured in an SEM are nonconductive. It is well known that nonconductive samples under electron irradiation cannot keep their original electric potential and “charge-up.” The type of charge (+ or -) and amount of charge depends on the sample, the electron beam, and the electro-magnetic fields around the sample. Even if charge equilibrium can be achieved, sample charging remains a dynamic process and slight changes in instrument parameters can alter the charge balance and result in apparent charging. Charge modeling is the second component needed in Path 2 (Fig. 1) discussed above. Charging is a highly variable part of the measurement process, and can introduce significant measurement errors. Davidson and Sullivan ('97), Ko *et al.* ('98), Fabrizio *et al.* ('93), Kotera and Suga ('88) and Grella *et al.* ('94) developed MC codes for taking sample charging into account for IC dimensional metrology applications. Davidson and Sullivan ('97) used the MC method to determine the amount and nature of charging under many instrumental conditions and were able to predict beam deflection of several

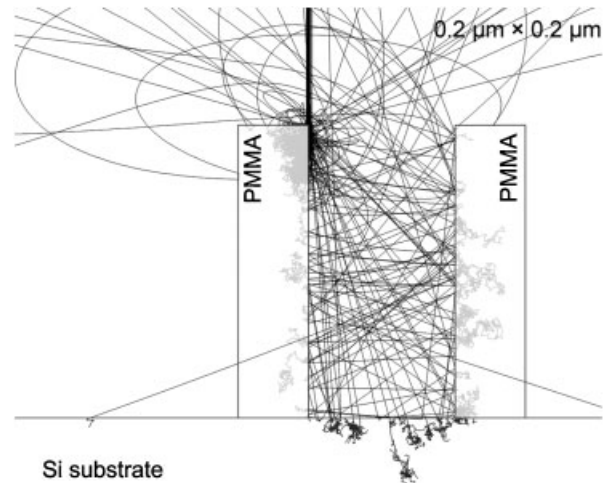


Fig 10. NIST JMonel MC Program calculated the trajectories of 100 electrons on a charging sample of PMMA structures on Si substrate. Note the curved trajectories due to charging. PMMA, poly(methyl methacrylate); MC, Monte Carlo.

nanometers on charging samples. This is consistent with the early experimental evidence presented by Postek ('84) on photomasks. Severe charging can deflect the electron beam to such an extent that it inhibits any repeatable measurement. Clearly, coating the sample with a very thin, but conductive layer of osmium, gold, or carbon can minimize that problem, but that is not always possible. Another possibility for charge reduction is the use of a variable-pressure SEM that in low-pressure gaseous environment around the sample diminishes the charge build-up (Postek and Vladár, 2003). In addition, the application of retarding or accelerating electric fields around the sample also can reduce the effects of sample charging. These fields can be readily incorporated into an MC model; other implementations are more sophisticated and take into account the charge conditions within the sample itself. Figure 10 shows trajectories of 100 electrons on a charging sample of poly(methyl methacrylate) or PMMA structures on a silicon substrate. Note the curved trajectories due to the charging (Villarrubia, 2011).

### Three-Dimensional Modeling

3D modeling properly accounts for all aspects of the sample (X, Y, and Z), including dealing with the corners which are often incorrectly represented when an X linescan and a Y linescan are summed. 3-D modeling is still in its infancy but early 3-D modeling has shown encouraging results. Some early work was published by Radzimksi and Russ ('95) of 3-D SEM BSE image results. The model was capable of computing various gold structures on a silicon substrate and showing the results in a 3D view, with proximity effect, and varying yields at all

sides. The results are convincing approximations. But, no experimental measurement comparison was made available. Other notable early 3D Monte Carlo-based modeling includes the work of Kotera *et al.* ('94) where a silicon sphere was modeled, and both backscattered and SE images were generated. The SE detector was modeled above the sample to simulate an in-lens detector and the BSE detector to the right, above the sample. The resulting modeling provided a convincing modeled analog of the actual structure. Improvements in a 3D code for more complicated samples and higher speed were published by Seeger *et al.* (2003). Seeger developed optimized ways for very fast codes and his codes performed orders of magnitude faster than the rigorous NIST MONSEL code.

New MC models for SEM dimension metrology (Villarrubia *et al.*, 2007) are generally more accurate than older ones, use the latest understanding of the fine details of electron–solid-state interaction and SE generation, and work well on features as small as 30 nm (Villarrubia, 2011). The efforts to make these programs even more accurate are underway. One example of the new model is the rigorous, accurate JMONSEL Monte Carlo simulation modeling method (Villarrubia, 2011). JMONSEL is a new 3-D code that can be used for accurate measurements and for the creation of the images that show proximity effects in SE generation and collection. Although JMONSEL can generate images also, it is inherently much slower than analog simulations (discussed below) because of the embedded physics and the number of electrons that must be individually tracked. But, it is now fast enough to be implemented in any metrology SEM, including CD-SEMs. JMONSEL is leading the way to the ability for accurate, model-based methods to be incorporated into all dimensional metrology SEMs.

### Analog Modeling

Analog instrument characterization modeling is the third component of Path B as described in the introduction. This is a combination of the simulated imaging concept described above and the instrument-modeling concept of DTSA. Analog modeling uses sophisticated pattern generation and various instrument parameters to account for factors related to instrument errors in the imaging and metrology process. Using the signal transactions on various sample features of real images or of rigorous MC calculations, the quality of the match of artificial images and real ones can be increased. Analog programs such as ARTIMAGEN (Cizmar *et al.*, 2007, 2008a,b, 2010) can generate hundreds of high

pixel-resolution SEM images in a matter of minutes. Essentially any type of sample can be defined, but it is especially useful and easy to use for semiconductor chip and mask patterns. Instrument test samples such as gold-on-carbon resolution sample structures can also be modeled. The generated images closely mimic the noise, contrast and resolution, drift, vibration and all other pertinent parameters of any SEM and allow for properly optimized measuring plans ensuring the correct instrument data will be collected at the highest throughput. The main advantage of the artificial image generation is that all the effects are deterministic and thus perfectly repeatable. None of these effects are either totally repeatable or deterministic with real SEM images.

Computational SEM through rapid artificial image modeling is gaining importance. It is a useful tool for the evaluation of imaging and metrology methods, because the repeatability of real SEMs is limited. The artificial image generator is capable of modeling the important instrument and perturbing effects in a deterministic way. One can *a priori* choose the drift function, the magnitude and type of the noise, the shape, size and charge distribution of the charged particle beam, etc. The computer-generated artificial images can be used as input to the imaging and metrology techniques and the results compared with the well-known parameters, hence reliably compare the performance of the various methods. This is impossible with the real images, where these effects are present, but all are unsystematic to some extent and often even entirely unknown.

### Conclusions

Monte Carlo modeling will become an ever increasing component of accurate dimensional metrology with the SEM. The modeling software for SEM metrology will comprise at least three, somewhat distinct components: The first is the input parameter section, the second and the key part contains the details of the physics implemented, and the last component is the visualization of the results. The form of the input is important for two reasons: it must be easy to work with, i.e. simple in the way the sample structures are entered, flexible in setting up parameter ranges and capable of translating the structure to be modeled into information that the second part could work with efficiently. From a simple text file to a complex 3D representation including powerful computer-aided design (CAD) software, the possibilities vary, and their usefulness depends on a number of characteristics. Those that allow for intuitive and interactive interface are superior, especially for 3D work.

The second part is the computation engine and this is where various Monte Carlo implementations vary greatly. The implanted ideas, shortcuts, approximations, and the physics of the electron and solid-state interaction will determine the speed, accuracy, and validity of the results. This is the part where the usefulness of the MC program is determined, and this is the part where X-ray, backscattered and secondary or TE, or electron-beam-induced current or conductivity and sample charging implementations vary from each other. The knowledge about various aspects and details of how to achieve more accurate results has grown over time and today's methods are significantly better than early programs. Luckily, even simple improvements such as not following every single primary electron with its energy and exact location at all locations within the sample, but calculating only an overall yield of SEs can provide valuable results in a shorter time. This has helped early MC applications and also the implementation of very fast codes that within a limited set of samples and parameters offer useful results quickly. But, speed is not free; the price for fast codes is reduced accuracy. This second part of the modeling also includes as sub-programs analog or MC instrument modeling to account for detrimental instrumental contributions to the data as well as an integrated charging model.

The third component of the model is an effective way to display the data. This is now often a separate (set of) software, and depending on sophistication, it can be a weakness or quite powerful, especially in 3D modeling. It is very important to get this part right, because human perception and interpretation of the results does not work well just by looking at a large set of numbers. Proper visualization and presentation is essential part of modeling.

Finally, between each of these three main components, a standardized data exchange interface should be developed and shared so that different modelers can easily compare their codes by “plugging-in” their particular components. This would be, in principle, similar to the algorithm checking with the artificial images described above.

Perhaps, the most important advantage of 1D and 2D modeling is the ability to achieve excellent dimensional metrology results, even in the realm of sub-nanometer measurement resolution, and with much better repeatability and accuracy than is possible without modeling. This is especially important in semiconductor production where it has been estimated that the economic value of reduced dimensions of ICs is measured in billions of dollars per a single nanometer (Ausschnitt and Lagus, '98). Additionally, SEM image simulation methods allow for better comparisons of designed and fabricated IC structures by the analysis of their SEM images, which makes improved design and better process control possible.

## Acknowledgements

The authors would like to thank Dr. David C. Joy for his dedication and significant contributions to the fundamental understanding and use of MC modeling for X-ray microanalysis and SEM dimensional metrology.

## References

- Ausschnitt CP, Lagus ME. 1998. Seeing the forest for the trees: a new approach to CD control. *Proc SPIE* 3332: 212–220.
- Bishop H. 1976. E: Monte Carlo simulations. In: Heinrich KFJ, *et al.*, editor. Use of Monte Carlo calculations in electron probe microanalysis and scanning electron microscopy, Vol. 460. NBS Special Publication. p 5–15.
- Cizmar P, Vladár AE, Postek MT. 2007. Image simulation for testing of SEM resolution measurement methods. *Scanning* 29:81–82.
- Cizmar P, Vladár AE, Ming B, Postek MT. 2008a. Artificial SEM images for testing resolution-measurement methods. *Microsc Microanal* 14:910–911.
- Cizmar P, Vladár AE, Ming B, Postek MT. 2008b. Simulated SEM images for resolution measurement. *Scanning* 30: 381–391.
- Cizmar P, Vladár AE, Postek MT. 2010. Advances in modeling of scanning charged-particle-microscopy images. *Proc SPIE Adv Lithogr* 7729:77290Z–772919Z.
- Czyzewski Z, Joy DC. 1989. A fast Monte Carlo for electron scattering in solids. *J Microsc* 156:285–292.
- Davidson MP, Sullivan N. 1997. An investigation of the effects of charging in SEM based CD metrology. *SPIE* 3050:226–242.
- Davidson MP, Vladár AE. 1999. An inverse scattering approach to SEM line width measurements. *SPIE Conference on Metrology, Inspection, and Process Control for Microlithography XIII*, Santa Clara, CA, SPIE Vol. 3677, 0277–786.
- Drouin D, Hovington P, Gauvin R. 1997. CASINO: a new era of Monte Carlo code in C language for the electron beam interaction—Part II: tabulated values of Mott cross section. *Scanning* 19:20–28.
- Drouin D, Couture AR, Joly D, Tastet X, Aimez V, Gauvin R. 2007. CASINO V2.42—a fast and easy-to-use modeling tool for scanning electron microscopy and microanalysis users. *Scanning* 29:92–101.
- Everhart TE, Chung MS. 1972. Idealized spatial emission distribution of secondary electrons. *J Appl Phys* 43: 3707–3711.
- Everhart TE, Hoff PH. 1971. Determination of kilovolt electron energy dissipation vs. penetration distance in solid materials. *J Appl Phys* 42:5837–5846.
- Fabrizio E, Grella L, Luciani L, Gentili M, Bacionchi M, Figilomeri M, Mastrogiacomo L, Maggiore R, Leonard Q, Cerrina F, Molino M, Powderly D. 1993. Metrology of high-resolution resist structures on insulating substrates. *J Vac Sci Technol B* 11:2456–2462.
- Farrow RC, Postek MT, Keery WJ, Jones SN, Lowney JR, Blakey M, Fetter L, Hopkins LC, Huggins HA, Liddle JA, Novembre AE, Peabody M. 1997. Application of transmission electron detection to SCALPEL mask metrology. *J Vac Sci Technol B* 15:2167–2172.
- Fiori C, Swyt C, Myklebust R. 1991. Desktop Spectrum Analyzer (DTSA), a comprehensive software engine for electron-excited X-ray spectrometry. Gaithersburg, MD: National Institute of Standards and Technology;

- Standard Reference Data Program; available from the following World Wide Web site: <http://www.cstl.nist.gov/div837/Division/outputs/software.htm>.
- Gorelikov DV, Remillard J, Sullivan NT, Davidson M. 2005. Model-based CD-SEM metrology at low and ultralow landing energies: implementation and results for advanced IC manufacturing. *Surf Interface* 37: 959–965.
- Green MA. 1963. Monte Carlo calculation of the spatial distribution of characteristic X-ray production in a solid target. *Proc Phys Soc* 82:204–215.
- Grella L, Fabrizio E, Massimo G, Baciocchi M, Mastrogiacomo L, Maggiora R. 1994. Secondary electron line scans over high resolution resist images: theoretical and experimental investigation of induced local electrical field effects. *J Vac Sci Technol B* 12:3555–3560.
- Hasselbach F, Rieke U, Straub M. 1983. An imaging secondary electron detector for the scanning electron microscope. *Scanning Electron Microscopy*. AMF O'Hare, IL: SEM Inc. p 467–478.
- Hatsuzawa TA. 1993. Cylindrical envelope projection model for estimation of secondary electron intensity distribution at micro-steps. *Meas Sci Technol* 4:842–845.
- Heinrich KFJ, Newbury DE, Yakowitz H. 1975. Use of Monte Carlo calculations in electron probe microanalysis and scanning electron microscopy. NBS Special Publication 460. p 1–164.
- Hovington P, Drouin D, Gauvin R. 1997. CASINO: a new era of Monte Carlo code in C language for the electron beam interaction—Part I: description of the program. *Scanning* 19:1–14.
- Joy D. 1995. Monte Carlo modeling for electron microscopy and microanalysis. NY: Oxford University Press. 216p.
- Joy DC. 1982. A Monte Carlo simulation for analytical electron microscopy. *Proceedings of the 40th EMSA Meeting*. Baton Rouge: Claitor's Press. p 746–747.
- Joy DC. 1984. Monte Carlo studies of high resolution secondary imaging. *Microbeam analysis*. San Francisco: San Francisco Press. p 81–82.
- Joy DC. 1986a. Image modelling for SEM-based metrology. In: Bailey GW, editor. *Proceedings of the 44th EMSA*. San Francisco: San Francisco Press. p 650–651.
- Joy DC. 1986b. Image modeling for SEM-based Metrology. In: Bailey GW, editor. *Proceedings of the Joint Annual Meeting EMSA/MAS*. San Francisco: San Francisco Press.
- Joy DC. 1989. A model for secondary and backscattered electron production. *J Microsc* 147:51–54.
- Joy DC. 1991. An introduction to Monte Carlo Simulations. *Scan Microsc* 5:329–337.
- Joy DC, Newbury DE, Myklebust RL. 1982. Role of fast secondary electrons in degrading spatial resolution in AEM. *J Microsc* 128:RP1.
- Ko YU, Chung MS, Kim SW. 1998. Monte Carlo simulation of charging effects on linewidth metrology. *Scanning* 20: 447–455.
- Kotera K, Suga H. 1988. A Simulation of keV electron scatterings in a charged-up specimen. *J Appl Phys* 63: 261–268.
- Kotera M, Yamaguchi S, Umegaki S, Suga H. 1994. Analysis of charging effect during observation of trench structures by scanning electron microscope Japan. *J Appl Phys* 33: 7144–7147.
- Kyser DF. 1981. Monte Carlo calculations for electron microscopy, microanalysis and microlithography. *Scanning Electron Microscopy/1981/I* 47-62 SEM, Inc., AMF O'Hare, IL.
- Kyser DF, Neidrig H, Newbury D, Shimizu R. 1982. Electron beam interactions with solids for microscopy, microanalysis and microlithography. AMF O'Hare, IL: SEM, Inc. 372p.
- Liddle JA, Blakey MI, Saunders T, Farrow RC, Fetter LA, Knurek CS, Novembre AE, Peabody ML, Windt DL, Postek MT. 1997. Metrology of SCALPEL masks. *J Vac Sci Technol B* 15:2197–2203.
- Lowney J. 1995a. MONSEL-II: Monte Carlo simulation of SEM signals for linewidth metrology. *Microbeam Anal* 4:131–136.
- Lowney J. 1995b. Use of Monte Carlo modeling for interpreting scanning electron microscope linewidth measurements. *Scanning* 17:281–286.
- Lowney J. 1996a. Application of Monte Carlo simulations to critical dimension metrology in a scanning electron microscope. *Scan Microsc* 10:667–678.
- Lowney J. 1996b. Monte Carlo simulation of scanning electron microscope signals for lithographic metrology. *Scanning* 18:301–306.
- Lowney J, Marx E. 1994. User's manual for the program MONSEL-I: Monte Carlo simulation of SEM signals for linewidth metrology. NIST Special Publication 400–95. Washington, DC: U. S. Government Printing Office. 41p.
- Lowney JR, Postek MT, Vladár AE. 1995a. Workshop report 2: Monte-Carlo models for predicting edge positions from scanning electron microscope signals. In: Edgar Etz, editor. *MAS Proceedings*, Cambridge University Press. p 341–342.
- Lowney JR, Postek MT, Vladár AE. 1995b. Workshop report 3: Edge positions from scanning electron microscope signals by comparing models with measurements. In: Edgar Etz, editor. *MAS Proceedings*, Cambridge University Press. p 343–344.
- Lowney JR, Postek MT, Vladár AV. 1996. A Monte Carlo model for SEM linewidth metrology. *Proc SPIE* 2196:85–96. *Metrologix*. Available at: <http://www.thefreelibrary.com/KLA+enters+SEM+metrology+market+with+acquisition+of+Metrologix.-a015981362>.
- Moll S, Healey F, Sullivan B, Johnson W. 1978. A high efficiency, non-directional backscattered electron detector mode for the SEM. *SEM/1978/I*. AMF O'Hare, IL: SEM, Inc. p 330–340.
- Moll S, Healey F, Sullivan B, Johnson W. 1979. Further developments of the converted backscattered electron detector. *SEM/1979/II*. AMF O'Hare, IL: SEM, Inc. p 149–154.
- Moore GE. 1965. Cramming more components into integrated circuits. *Electronics* 38:114–119.
- Moore GF. 1995. Lithography and the future of Moore's Law. *Proc SPIE* 2437:2–17.
- Myklebust R, Newbury D, Yakowitz H. 1976. NBS Monte Carlo Electron Trajectory Calculation Program. In: Heinrich K, Newbury D, Yakowitz H, editors. NBS Special Publication 460. Washington, DC: U. S. Government Printing Office. p 105–125.
- Nyssonen DA. 1988. New approach to image modeling and edge detection in the SEM. *SPIE Proceedings* 921:48–56.
- Peters KR. 1982. Conditions required for high quality high magnification images in secondary electron scanning electron microscopy. *SEM/1982/IV*. AMF O'Hare, IL: SEM Inc. p 1359–1372.
- Peters KP. 1985. Working at higher magnifications in scanning electron microscopy with secondary and backscattered electrons on metal coated biological specimens and imaging macromolecular cell membrane structures. *Scanning Electron Microscopy*. AMF O'Hare, IL: SEM Inc. p 1519–1544.
- Postek MT. 1984. Low accelerating voltage inspection and linewidth measurement in the scanning electron microscope. *SEM/1984/III*. AMF O'Hare, IL: SEM, Inc. p 1065–1074.
- Postek MT, Keery WJ, Larrabee RD. 1988. The relationship between accelerating voltage and electron detection

- modes to linewidth measurement in the SEM. *Scanning* 10:10–18.
- Postek MT. 1990. Low accelerating voltage SEM imaging and metrology using backscattered electrons. *Rev Sci Instrum* 61:3750–3754.
- Postek MT, Joy DC. 1987. Submicrometer microelectronics dimensional metrology: scanning electron microscopy. *NBS J Res* 92:205–228.
- Postek MT, Vladár AE. 2003. Application of high pressure/environmental electron microscopy for photomask dimensional metrology. In: Seiler D, *et al.*, editor. CP 683 Characterization and Metrology for ULSI Technology: 2003 International Conference. New York: AIP Press. p 396–399.
- Postek MT, Larrabee RD, Keery WJ 1989. A new approach to accurate X-ray mask measurements in a scanning electron microscope. *IEEE Trans Electron Dev* 36:2452–2457.
- Postek MT, Vladár AE, Jones S, Keery WJ. 1993a. Interlaboratory study on the lithographically produced scanning electron microscope magnification standard prototype. *NIST J Res* 98:447–467.
- Postek MT, Lowney JR, Vladár AE, Keery WJ, Marx E, Larrabee RD. 1993b. X-ray lithography mask metrology: use of transmitted electrons in an SEM for linewidth measurement. *NIST J Res* 98:415–445.
- Postek MT, Vladár AE, Banke GW, Reilly TW. 1995. Workshop Report 1: Scanning electron microscope metrology as related to a defined edge structure. In: Edgar Etz, editor. MAS Proceedings, Cambridge University Press. p 339–340.
- Postek MT, Vladár AE, Lowney JR, Keery W. 2002. Two-dimensional simulation and modeling in scanning electron microscope imaging and metrology research. *Scanning* 24:179–185.
- Radzimski ZJ, Russ J. 1995. Image simulation using Monte Carlo methods: electron beam and detector characteristics. *Scanning* 17:276–280.
- Radi Z, Vladár AE, Postek MT. 2003. Information transfer capability and signal processing performance of modern scanning electron, microscopes. *Microsc Microanal* 9:762–763.
- Ritchie NWM. 2011. Getting started with NIST DTSA – II. *Microsc Today* 19:26–31.
- Seeger A, Fretzagias Ch, Taylor R. 2003. II Software acceleration techniques for the simulation of scanning electron microscope images. *Scanning* 25:264–273.
- Villarrubia JS. 2011. NIST JMonSel with the addition of sample charging modeling capability, Private communication.
- Villarrubia JS, Vladár A, Lowney J, Postek MT. 2001. Shape-sensitive linewidth measurement with the SEM using a model-based library. *Scanning* 23:90–91.
- Villarrubia J, Vladár AE, Lowney JR, Postek MT. 2003. Comparison of model-based library SEM measurements to cross sections. *Scanning* 25:73–74.
- Villarrubia JS, Vladár AE, Postek MT. 2005. Scanning electron microscope dimensional metrology using a model-based library. *Surf Interface Anal* 37:951–958.
- Villarrubia JS, Ritchie NWM, Lowney JR. 2007. Monte Carlo modeling of secondary electron imaging in three Dimensions, Metrology, Inspection, and Process Control for Microlithography XXI. In: Archie CN, Proceedings of SPIE, Vol. 6518, 65180K. p 277–786.